Molecular Imaging and Local Density of States Characterization at the Si(111)/NaOH Interface

P. Allongue*

Laboratoire de Physique des Liquides et Électrochimie, Laboratoire associé à l'ESPCI, 10 rue Vauquelin, Bat. H, F-75005 Paris, France

We present *in situ* scanning tunneling microscopy (STM) images with the resolution of isolated $\equiv$Si—OX groups on H-Si(111) in NaOH solutions with or without isopropyl alcohol [$X = H$ or —CH(CH$_3$)$_2$]. The comparison of STM with geometric contours shows that the electronegativity of OH ligands enhances the local density of states and generates a surface potential distribution. The dependence of both observations with the radical X and the mechanisms of grafting are discussed. [S0031-9007(96)00973-8]

The downsizing and increased integration of electronic components demands ever greater attention to the compositional and structural homogeneity of the surface of semiconductor wafers after etching. As such, the study of silicon surface morphology and composition is an area of great technological importance [1]. Silicon etching in aqueous media, such as HF and alkaline solutions, leaves the surface almost entirely passivated by Si—H bonds [2,3]. From a structural point of view, the flattest surfaces, at the atomic scale, are obtained by etching (111) wafers in buffered ammonium fluoride of pH 8, while facetting occurs on the (100) face in the same solution [1,4]. Experimentally, the doping of the substrate [5] as well as the surface misorientation [6–8] are, however, critical parameters to obtain ordered (111) surfaces. Highly doped p-type substrates give rough surfaces [5]. Precisely oriented low doped n- and p-(111) samples are always left with triangular etch pits after treatment [5,6], while vicinal surfaces (tilted by few degrees) may have a staircase structure after etching [6,7]. Decreasing the pH of the etching solution roughens (111) surfaces at the atomic scale, and smooth terraces are no longer observable [9–11].

The molecular model shown in Fig. 1 [11] accounts for most of the above observations. It particularly states that Si "chemical etching" comprises two components, one electrochemical (free carrier involved) and the other chemical (no free carrier involved). After the primary substitution reaction Si—H → Si—OH, the sequence of chemical steps is fast because the difference in electronegativity, between the Si surface atom and its ligand, favors the attack at back bonds. For steric reasons the chemical route is highly anisotropic and occurs almost exclusively at steps (Fig. 1, top route). The electrochemical path is conversely relatively isotropic and may occur on (111) planes since the first dissociative step leaves the space necessary to the second reaction with water molecule (Fig. 1, bottom route). The surface microstructure of "chemically etched" Si(111) is therefore closely related to the partition between the two pathways [11], and flat Si(111) surfaces are obtainable in conditions (pH, doping level, type of conduction, etc.) such that the electrochemical route is almost suppressed so as to make the dissolution anisotropic.

Despite a large amount of correlation, the precursors of the dissolution of silicon, i.e., Si—OH groups, have, however, never been directly imaged by scanning tunneling microscopy (STM) [1,4,6,8–12], nor unambiguously detected by Fourier-transform infrared (FTIR) spectroscopy [1–3,7,10]. This paper presents the first STM observations of isolated vertical $\equiv$Si—OH on Si(111) in contact with an aqueous solution and discusses the local changes in the electronic properties induced by the silanol group. In the presence of isopropyl alcohol (IPA), an additive frequently used in Si etching [13], $\equiv$Si—OR bond formation also occurs [$R = $ —CH(CH$_3$)$_2$] and images show that the electronegativity and the molecular arrangement of the ligand are critical parameters to the local electronic properties of the surface.

In situ constant current STM images were acquired in 2M NaOH with a home built microscope operating in the four-electrode configuration [14]. All images were acquired with the sample potential $U_{\text{sample}} \sim$ −0.57 V/Pd—H (quasi-Pd hydrogen reference electrode) so as to accumulate electrons at the surface and allow long standing imaging [12]. This situation also avoided fast etching [14] because of the evolution
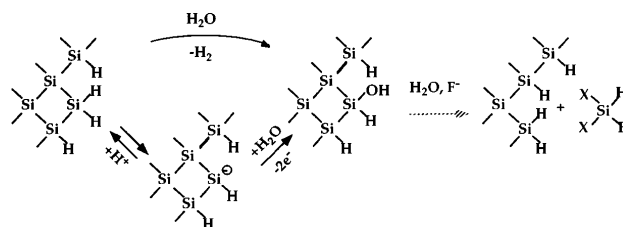

FIG. 1. Molecular model for Si etching in aqueous solutions. The reaction is either chemical (top route) or electrochemical (bottom route) in initial stages. For steric reasons, formation of $\equiv$Si—OH on (111) plane stems from the bottom reaction. Reactants are shown with (+) and reaction products with (−). See Ref. [11] for more details.

of hydrogen (typical current $\sim 300\ \mu A/cm^2$). The tip potential was $U_{tip} \sim 0.3$ V/Pd—H. The tunnel voltage $U_{tunnel} = U_{sample} - U_{tip}$ was therefore -0.75 V (sample negative) and the tunnel current 0.2 nA in all images. A Pt wire was used as auxiliary electrode to collect the electrochemical current issued from the sample surface. Si(111) samples (0.5Ω cm n-type) were degreased in a sequence of hot solvents before stripping the oxide in 40% HF (1 min) and etching in 40% NH_4F (3 min). The rear Ohmic contact was made with In-Ga alloy.

Figure 2 shows the effect of pulsing U_{sample} from -0.57 V/Pd—H (cathodic region) to ~ 0 V/Pd—H for 5 s, which is nearly the rest bias. Top and bottom images were recorded at $U_{sample} = -0.57$ V/Pd—H while the pulse of potential was applied between the two frames using a special procedure [14]. The differences between top and bottom images correspond, therefore, to a short chemical etching of the surface. Images are presented as unfiltered top views. In left images heights decrease from white to black, and the successive atomic planes, all separated by a single bilayer step (3.1 Å high), appear with different colors. Under prolonged cathodic polarization (top), only a very slow etching process was observable at step edges. Using the procedure in Ref. [14], the etch rate was found to be 0.2 Å/min. After the pulse of potential, the growth of some existing pits (e.g., site A) and the nucleation of new ones (e.g., site B) were also observed in addition to a faster motion of steps. The etch rate was ~ 5 Å/min during the 5 s chemical etching.

In the right images of Fig. 2, the full grey scale has been applied to each of the terraces to resolve that they present shallow defects whose depth and diameter are, respectively, nearly 1 Å and ~ 30 Å. Observations were similar of other places and on other samples using different tips. Different types of such sites can be identified: (i) sites which exist before and after the pulse (site C), (ii) sites which give rise to a pit (site D), and (iii) sites which are newly formed (site E). On several instances the density of shallow defects N was measured to be $\sim 1 - 2 \times 10^{11}/cm^2$ before the pulse (Fig. 2, top), and was about twice as large after the pulse (Fig. 2, bottom). By comparison N remained nearly constant under prolonged hydrogen evolution.

At high resolution the surface is entirely (1×1) H-terminated [3,14] except for a few irregularities, as shown in Fig. 3. Irregularities are depressions of diameter 10–20 Å, comparable to the diameter of former defects (Fig. 2), with a central atom, however, resolved. Vertically the protrusion is ≥ 0.5 Å above the average corrugation of Si—H bonds. The density of defects is ca. 5×10^{12} cm^{-2} in this image, which is larger than in Fig. 2 where the solution was poorer.

As such, Fig. 2 clearly shows that the nucleation of etch pits (left column) and the bias dependence of N (right column) are related to the electrochemical route in Fig. 1 (bottom) because its onset coincides with the rest bias [11]. The second point suggests, therefore, that the depressions on terraces are vertical $\equiv$Si—OH bonds since their formation precedes the removal of the Si atoms in Fig. 1. Figure 2 demonstrates that isolated $\equiv$Si—OH are relatively stable on terraces and that their density remains nevertheless less than 1% of a monolayer, which explains that a "full" H-termination of the surface
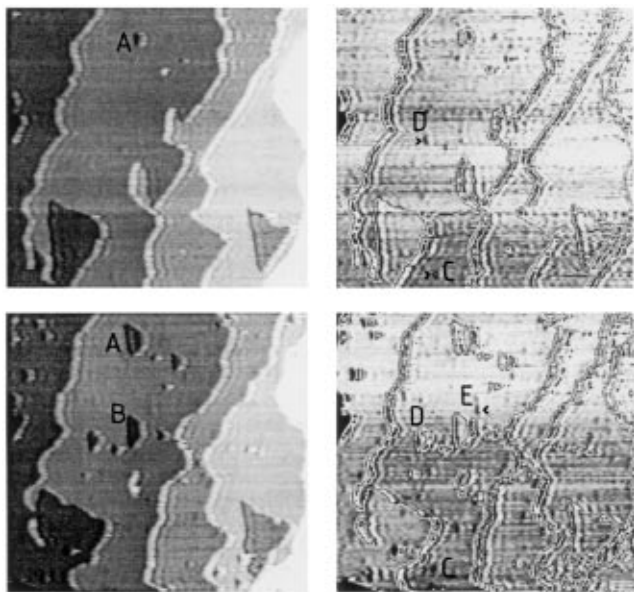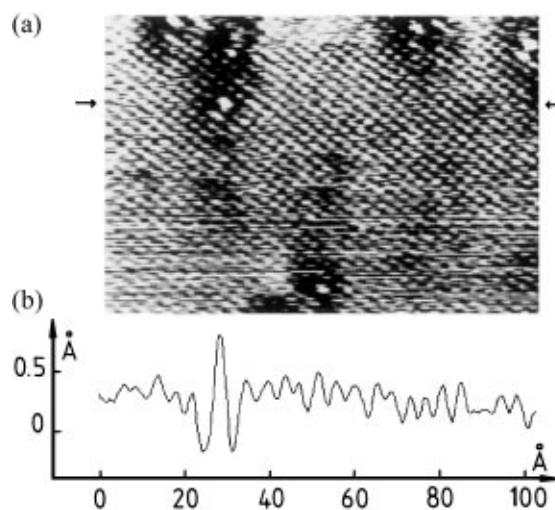

FIG. 2. *In situ* STM images of n-Si(111) in NaOH. Top: after prolonged cathodic polarization. Bottom: after pulsing the sample potential so as to reach the rest bias for 5 s (i.e., "chemical etching" conditions). Left and right images correspond to different representation of the same portion of the surface (see text). See text for identification of the sites $A-E$. Frames are 1400×1400 Å^2. $i_{tunnel} = 0.2$ nA and $U_{tunnel} = -0.72$ V.

FIG. 3. (a) Atomic structure of the surface showing few isolated $\equiv$Si—OH sites (frame 103×70 Å^2). (b) Cross section of the site marked by an arrow. $i_{tunnel} = 0.2$ nA and $U_{tunnel} = -0.79$ V.

was inferred from FTIR spectroscopy [1–3,7,10]. That only 10% of existing $\equiv$Si—OH groups give birth to a pit after the pulse (see, e.g., site D in Fig. 2) is direct evidence of the large energy barrier for Si anisotropic etching [15], and is also an experimental verification of recent Monte Carlo simulation [16,17], which suggest that *several* OH, next to each other, are necessary to initiate an etch pit. Step edge Si atoms are by comparison removed as soon as the Si—OH bond is formed [11,16].

In a mixture of isopropyl alcohol (IPA) in NaOH, two types of sites were resolved at the atomic level. Most of them, labeled as A, in Fig. 4, looked significantly different from those observed in Fig. 3. They consisted of a 0.3 Å high protrusion with no darker ring around. Observations were quite similar on other samples in the same solution. The other irregularities in Fig. 4 (designated as B) presented the characteristic depression region seen in Fig. 3, even though the central protruding atom is not always clearly resolved in this image.

Tunneling conditions being nearly identical throughout this study [18], the differences between irregularities seen in Figs. 3 and 4 cannot be attributed to changes in tip-sample distance or interactions. That the same differences are seen on the same surface (Fig. 4) is a further proof. In analogy with the discussion about $\equiv$Si—OH sites, it is realistic to associate sites (A) of Fig. 4 with $\equiv$Si—OR $[R = -CH(CH_3)_2]$ surface groups, while sites (B) are $\equiv$Si—OH as in Figs. 2 and 3. An electrochemical reaction similar to the one in Fig. 1 (bottom), but involving R—OH molecules instead of H—OH molecular water, is indeed quite realistic [19]. This second reaction competes with the one in Fig. 1 (top) and explains that sites (A) and (B) may coexist on the same surface (Fig. 4).
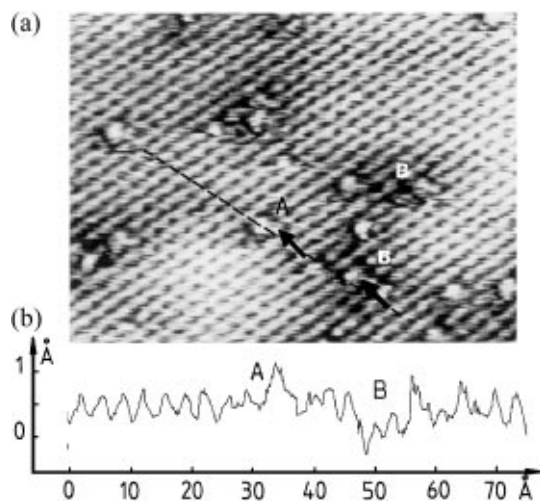
Images being recorded in the constant current mode, the comparison of electronic contours of occupied states in Figs. 3 and 4 with hard sphere molecular models (Fig. 5) yields information regarding the local electronic properties at $\equiv$Si—OX (X = H, R). In the case of $\equiv$Si—OH groups the excess height of STM contours (by $\geq$0.2 Å) means an enhanced local density of states (LDOS), and the depressed region around indicates a tunnel bias locally smaller [the tunnel current varies as $(U_T/s)N_s \exp(-Ks)$, with U_T the tunnel bias, N_s the LDOS, and s the tip to sample separation]. In the case of $\equiv$Si—OR sites, the STM height is conversely smaller than expected (by 1.4 Å). No variation of U_T is observed in this case.

We discuss first the local variations of the tunnel bias. Given the band diagram of the tunnel junction [14], a local decrease of U_T means a lowering of the conduction band edge minimum (in the energy scale) from where electrons are tunneling into the tip. In other words, darker regions in Figs. 2–4 originate from a 3D potential well. Even though the exact distribution of the electronic cloud is more complex at a molecule attached to a surface than at an isolated molecule, considering the system $\equiv$Si$^{+\delta}$—O$^{-\delta'}$—X$^{+\delta''}$ yields sufficient insights into the interpretation of images. Assuming that $\delta' \sim \delta''$, the charge δ on $\equiv$Si$^{+\delta}$ increases as the electronegativity difference between the oxygen and the group X. Taking $E_R \sim 2.56$ as electronegativity of short alkyl chains [20] and $E_H = 2.1$ for H, δ increases according to the series $\equiv$Si—H $< \equiv$Si—OR $< \equiv$Si—OH since δ' increases from 0.19 to 0.39 if $X = R$ and H, respectively ($\delta \sim -0.02$ at $\equiv$Si—H). It can therefore be inferred that the potential distribution at ligands simply arises from the electric field induced by $+\delta$ since the depth of dark rings follows the same series $\equiv$Si—OR $< \equiv$Si—OH (Figs. 3 and 4). Similar band bending ef-
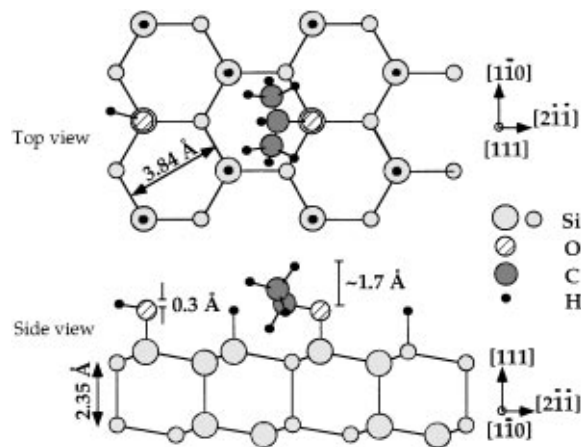

FIG. 4. Same as Fig. 3, but in a NaOH solution containing 10% IPA (frame 98 × 72 Å^2). Sites A and B are, respectively, $\equiv$Si—OR and $\equiv$Si—OH groups. (b) Cross section. $i_{tunnel} = 0.2$ nA and $U_{tunnel} = -0.82$ V.

FIG. 5. Atomic models of $\equiv$Si—OH and $\equiv$Si—OR $[R = -CH(CH_3)_2]$ groups attached on Si(111). Top and side views. Bond lengths were taken from chemical handbooks. Atom diameters were reduced to ease representation.

fects have been reported in the UHV, with oxygen adsorbed on GaAs(110) [21]. The amplitude of the STM corrugation and the screening distances were, however, much larger in the UHV than in this study where the effect is screened over few atomic distances (Figs. 2 and 3). Two effects combine here: a large density of ionic charges in solution and also the accumulation of electrons at the surface necessary to imaging [14] which both reduce electrostatic effects.

If the increased LDOS at $\equiv$Si—OH was anticipated (the LDOS is known to be smallest at $\equiv$Si—H[22]), other effects need to be considered in the case of $\equiv$Si—OR surface groups. According to the discussion about the charge δ on $\equiv$Si$^{+\delta}$, the LDOS should follow the same series $\equiv$Si—H $<$ $\equiv$Si—OR $<$ $\equiv$Si—OH, which seems in contrast to observations (the corrugation at $\equiv$Si—OR is shallower than expected in Fig. 4). Looking into more detail at Fig. 4, the maximum in the LDOS appears elongated and displaced toward the hollow site position, which is consistent with the fact that the R group is electron acceptor. The preferential orientation of the protrusion (A), along $\langle 1\bar{1}0 \rangle$, agrees also with the configuration of $\equiv$Si—OR in Fig. 5. The molecule is indeed expected to be most stable on the surface with the R group *above* the hollow site, with no Si atom immediately underneath. This not only minimizes steric interactions, but also likely pumps the electronic cloud downward, making the STM contour shallower than expected.

In conclusion, the precursor chemical states of Si etching have been imaged by *in situ* STM. In instances where IPA was added to the solution, molecular grafting has been also observed. The local electronic properties of the surface appear to be controlled by the ligand electronegativity. With increasing electronegativity the LDOS increases and a potential distribution is induced. The steric arrangement on the surface may, however, have a beneficial effect. Within this description the electronic passivation of H-terminated Si surfaces arises from the unpolar character of $\equiv$Si—H bonds. The results in the IPA solution suggest that Si surfaces might be also passivated by grafting a monolayer $\equiv$Si—OR groups (using a water free solvent).

*Electronic address: pa@ccr.jussieu.fr
FAX: +33 1 43 36 16 80

[1] G. S. Higashi and Y. J. Chabal, in *Handbook of Semiconductor Wafer Cleaning Technology,* edited by W. Kern (Noyes Publications, Park Ridge, NJ, 1993).

[2] A. Venkateswara Rao, F. Ozanam, and J.-N. Chazalviel, J. Electrochem. Soc. **138**, 153 (1991).

[3] J. Rappich, H. J. Lewerenz, and H. Gerischer, J. Electrochem. Soc. **141**, L187 (1994).

[4] Sueh-Lin, *et al.,* Appl. Phys. Lett. **66**, 766 (1995).

[5] J. F. Roche, M. Ramonda, F. Thibaudeau, Ph. Dumas, Ph. Mathiez, F. Salvan, and P. Allongue, Microscopy, Microstruct. and Microanal. **5**, 291–299 (1994).

[6] G. J. Pietsch, U. Köhler, and M. Henzler, J. Appl. Phys. **73**, 4797 (1993).

[7] P. Jakob and Y. J. Chabal, J. Chem. Phys. **95**, 2897 (1991).

[8] P. Allongue, V. Kieling, and H. Gerischer, J. Phys. Chem. **99**, 9472 (1995).

[9] H. E. Hessel, A. Feltz, U. Memmert, and R. J. Behm, Chem. Phys. Lett. **186**, 275 (1991).

[10] P. Jakob, Y. J. Chabal, K. Raghavachari, R. S. Becker, and A. J. Becker, Surf. Sci. **275**, 407 (1992).

[11] P. Allongue, V. Kieling, and H. Gerischer, Electrochim. Acta **40**, 1353 (1995); J. Electrochem. Soc. **140**, 1019 (1993).

[12] P. Allongue, in *Advances in Electrochemical Science and Engineering,* edited by H. Gerischer and C. W. Tobias (VCH Verlagesellschaft, Weinheim, 1995), Vol. 4, Chap. 1.

[13] J. B. Price, in *Semiconductor Silicon,* edited by H. R. Huff and R. R. Burgess, *Electrochem. Soc. Soft Bounds* (The Electrochemical Society, Princeton, NJ, 1973).

[14] P. Allongue, V. Kieling, and H. Gerischer, J. Electrochem. Soc. **140**, 1008 (1993); P. Allongue, H. Brune, and H. Gerischer, Surf. Sci. **275**, 414 (1992).

[15] M. Elwenspoek, J. Electrochem. Soc. **140**, 2075 (1993).

[16] P. Allongue and J. Kasparian, Microscopy, Microstruct. and Microanal. **5**, 357 (1994).

[17] P. Allongue (to be published).

[18] It was not possible to further substantiate observations by varying the tunnel bias $U_{tunnel} = U_{sample} - U_{tip}$ by more than 0.1–0.2 V; $U_{sample} \sim 0.57$ V/Pd—H was a good compromise to stabilize the surface without too strong H$_2$ evolution, and $U_{tip} \sim 0.3$ V/Pd—H was fixed to minimize the electrochemical current at its extremity. The tunnel current had no detectable effect in the range 0.2–1 nA. Above these values images were noisier.

[19] M. Warntjes, C. Veillard, F. Ozanam, and J. N. Chazalviel, J. Electrochem. Soc. **142**, 4138 (1995).

[20] R. J. Boyd and K. E. Edgecombe, J. Am. Chem. Soc. **110**, 4182 (1988).

[21] J. A. Strocio, R. M. Feenstra, and A. P. Fein, Phys. Rev. Lett. **58**, 1668 (1987).

[22] R. S. Becker, G. H. Higashi, Y. J. Chabal, and A. J. Becker, Phys. Rev. Lett. **65**, 1917 (1990).